HAL
open science

Investigating the two-moment characterisation of subcellular biochemical networks

Mukhtar Ullah, Olaf Wolkenhauer

To cite this version:

Mukhtar Ullah, Olaf Wolkenhauer. Investigating the two-moment characterisation of subcellular biochemical networks. Journal of Theoretical Biology, 2009, 260 (3), pp.340. 10.1016/j.jtbi.2009.05.022 . hal-00554615

HAL Id: hal-00554615

https://hal.science/hal-00554615v1

Submitted on 11 Jan 2011

HAL is a multi-disciplinary open access archive for the deposit and dissemination of scientific research documents, whether they are published or not. The documents may come from teaching and research institutions in France or abroad, or from public or private research centers.

L'archive ouverte pluridisciplinaire **HAL**, est destinée au dépôt et à la diffusion de documents scientifiques de niveau recherche, publiés ou non, émanant des établissements d'enseignement et de recherche français ou étrangers, des laboratoires publics ou privés.

Author's Accepted Manuscript

www.elsevier.com/locate/yjtbi

Investigating the two-moment characterisation of subcellular biochemical networks

Mukhtar Ullah, Olaf Wolkenhauer

PII: S0022-5193(09)00247-1
DOI: doi:10.1016/j.jtbi.2009.05.022
Reference: YJTBI 5577

To appear in: *Journal of Theoretical Biology*

Received date: 12 August 2008
Revised date: 13 May 2009
Accepted date: 23 May 2009

Cite this article as: Mukhtar Ullah and Olaf Wolkenhauer, Investigating the two-moment characterisation of subcellular biochemical networks, *Journal of Theoretical Biology*, doi:10.1016/j.jtbi.2009.05.022

This is a PDF file of an unedited manuscript that has been accepted for publication. As a service to our customers we are providing this early version of the manuscript. The manuscript will undergo copyediting, typesetting, and review of the resulting galley proof before it is published in its final citable form. Please note that during the production process errors may be discovered which could affect the content, and all legal disclaimers that apply to the journal pertain.

ACCEPTED MANUSCRIPT

Investigating the two-moment characterisation of subcellular biochemical networks

Mukhtar Ullah[a], Olaf Wolkenhauer[*,a,b]

[a] *Systems Biology and Bioinformatics Group, Department of Computer Science, University of Rostock, Albert Einstein Str. 21, 18051 Rostock, Germany*
[b] *Stellenbosch Institute for Advanced Study (STIAS), 10 Marais Street, Stellenbosch 7600, South Africa*

Abstract

While ordinary differential equations (ODEs) form the conceptual framework for modelling many cellular processes, specific situations demand stochastic models to capture the influence of noise. The most common formulation of stochastic models for biochemical networks is the chemical master equation (CME). While stochastic simulations are a practical way to realise the CME, analytical approximations offer more insight into the influence of noise. Towards that end, the two-moment approximation (2MA) is a promising addition to the established analytical approaches including the chemical Langevin equation (CLE) and the related linear noise approximation (LNA). The 2MA approach directly tracks the mean and (co)variance which are coupled in general. This coupling is not obvious in CME and CLE and ignored by LNA and conventional ODE models. We extend previous derivations of 2MA by allowing a) non-elementary reactions and b) relative concentrations. Often, several elementary reactions are approximated by a single step. Furthermore, practical situations often require the use relative concentrations. We investigate the applicability of the 2MA approach to the well established fission yeast cell cycle model. Our analytical model reproduces the clustering of cycle times observed in experiments. This is explained through multiple resettings of MPF, caused by the coupling between mean and (co)variance, near the G2/M transition.

Key words: Noise, two-moment approximation, mean, (co)variance, cell cycle

Accepted manuscript

1. Introduction

At a coarse level, cellular functions are largely determined by spatio-temporal changes in the abundance of molecular components. At a finer level, cellular events are triggered by discrete and random encounters of molecules [1]. This

*Corresponding author. Tel./Fax: +49 (0)381 4987570/72, URL: www.sbi.uni-rostock.de
Email addresses: `mukhtar.ullah@uni-rostock.de` (Mukhtar Ullah), `olaf.wolkenhauer@uni-rostock.de` (Olaf Wolkenhauer)

ACCEPTED MANUSCRIPT

suggests a deterministic modelling approach at the coarse level (cell function) and a stochastic one at the finer level (gene regulation) [2–11]. However, stochastic modelling is necessary when noise propagation from processes at the fine level changes cellular behaviour at the coarse level.

Stochasticity is not limited to low copy numbers. The binding and dissociation events during transcription initiation are the result of random encounters between molecules [4]. If molecules are present in large numbers and the molecular events occur frequently, the randomness would cancel out (both within a single cell and from cell to cell) and the average cellular behaviour could be described by a deterministic model. However, many subcellular processes, including gene expression, are characterised by infrequent (rare) molecular events involving small copy numbers of molecules [1, 4]. Most proteins in metabolic pathways and signalling networks, realising cell functions, are present in the range 10-1000 copies per cell [12–14]. For such moderate/large copy numbers, noise can be significant when the system dynamics are driven towards critical points in cellular systems which operate far from equilibrium [15–17]. The significance of noise in such systems has been demonstrated for microtubule formation [18], ultrasensitive modification and demodification reactions [12], plasmid copy number control [19], limit cycle attractor [20], noise-induced oscillations near a macroscopic Hopf bifurcation [21], and intracellular metabolite concentrations [22].

Noise has a role at all levels of cell function. Noise, when undesired, may be suppressed by the network (e.g. through negative feedback) for robust behaviour [2, 23–27]. However, all noise may not be rejected and some noise may even be amplified from process to process, and ultimately influencing the phenotypic behaviour of the cell [6, 11, 28–30]. Noise may even be exploited by the network to generate desired variability (phenotypic and cell-type diversification) [2, 31–34]. Noise from gene expression can induce new dynamics including amplification (stochastic focusing) [6, 35, 36], bistability (switching between states) and oscillations [37–40], that is both quantitatively and qualitatively different from what is predicted or possible deterministically.

The most common formulation of stochastic models for biochemical networks is the chemical master equation (CME). While stochastic simulations [41] are a practical way to realise the CME, analytical approximations offer more insights into the influence of noise on cell function. Formally, the CME is a continuous-time discrete-state Markov process [42–44]. For gaining intuitive insight and a quick characterisation of fluctuations in biochemical networks, the CME is usually approximated analytically in different ways [44, 45], including the frequently used the chemical Langevin approach [46–49], the linear noise approximation (LNA) [15, 50–52] and the two-moment approximation (2MA) [53–55].

Of the analytical approaches mentioned above, we here focus on the 2MA approach because of its representation of the coupling between the mean and (co)variance. The traditional Langevin approach is based on the assumption that the time-rate of abundance (copy number or concentration) or the flux of a component can be decomposed into a deterministic flux and a Langevin noise term, which is a Gaussian (white noise) process with zero mean and amplitude

Accepted manuscript

ACCEPTED MANUSCRIPT

determined by the the dynamics of the system. This separation of noise from the system dynamics may be a reasonable assumption for *external noise* that arises from the interaction of the system with other systems (like the environment), but cannot be assumed for internal noise that arises from within the system [4, 5, 11, 14, 56, 57]. As thoroughly discussed in [47], internal noise is not something that can be isolated from the system because it results from the discrete nature of the underlying molecular events. Any noise term in the model must be derived from the system dynamics and cannot be presupposed in an *ad hoc* manner. However the chemical Langevin equation (CLE) does not suffer from the above criticism because Gillespie [46] derived it from the CME description (see also [58]). The CLE allows much faster simulations compared to the exact stochastic simulation algorithm (SSA) [43] and its variants. The CLE is a stochastic differential equation (dealing directly with random variables rather than moments) and has no direct way of representing the mean and (co)variance and the coupling between the two. That does not imply that CLE ignores the coupling like the LNA which has the same mean as the solution of the deterministic model.

The merits of the 2MA compared to alternative approximations have been discussed in [53, 54, 59]. In [55], the 2MA is developed as an approximation of the master equation for a generic Markov process. In [54], the 2MA framework is developed under the name "mass fluctuation kinetics" for biochemical networks composed of elementary reactions. The authors demonstrate that the 2MA can reveal new behaviour like stochastic focusing and bistability. Another instance of the 2MA is proposed in [45, 53] under the names "mean-field approximation" and "statistical chemical kinetics". Again, the authors assume elementary reactions so that the propensity function is at most quadratic in concentrations. The authors evaluate the accuracy of the 2MA against the alternatives (such as LNA) for a few toy models. The derivation of the 2-MA for more general systems with non-elementary reactions is one motivation for the present paper.

The 2MA approaches referred to above assume absolute concentrations (copy number divided by some fixed system size parameter). In systems biology, however, models often use relative concentrations with arbitrary units [60–63]. In general, the concentration of each component in the system may have been obtained by a different scaling parameter, rather than using a global system size. For such models, the above mentioned approaches need modification. This was another motivation for our derivation in this paper.

In the present paper we develop a compact derivation of the first two-moments, the mean and (co)variance of the continuous-time discrete-state Markov process that models a biochemical reaction system by the CME. This derivation is an extension of previous derivations, taking into account arbitrary concentrations and non-elementary reactions. The matrix form of our derivation allows for an easy interpretation. Using these analytical results, we develop our 2MA model of the fission yeast cell cycle which has two sets of ODEs: one set for the mean protein concentrations and the other set for concentration (co)variances. Numerical simulations of our model show a considerably different behaviour. Especially, for the *wee1*$^-$ *cdc25*Δ mutant (hereafter referred simply as double-mutant), the timings of S-phase and M-phase are visibly different from those

Accepted manuscript

ACCEPTED MANUSCRIPT

obtained for a deterministic model because of the oscillatory behaviour of the key regulator. Since the 2MA is only an approximation, we investigate its validity by comparing the statistics computed from the 2MA model with experimental data.

The rest of this paper is organised as follows. In the first section we introduce the basic terminology and notation. Then the system of ODEs forming the 2MA approach is presented. Next, we introduce an application to the fission yeast cell cycle model [60]. We present a 2MA model of the cell cycle, followed by a comparison to the experimental data and conclusions. The appendices contain full derivations of the 2MA model, further proofs and additional tables.

2. Stochastic modelling of biochemical systems

Imagine a well-mixed homogeneous cellular compartment of a fixed volume V at thermal equilibrium that contains molecules of s different kinds (each kind referred to as a chemical *component* or *species*) interacting in r distinct ways (each way referred to as a reaction *channel* or *step*). Since these biochemical reactions occur by random encounters of reactant molecules, the copy number of a particular component present in the system at time t fluctuates. The state of the cellular system is described by the $s \times 1$ random vector $N(t)$ whose ith element is the copy number $N_i(t)$ of the ith species present in the system at time t. Each (time-varying) element $N_i(t)$ is a stochastic process, where $N_i(t) = n_i$ means that n_i molecules of the ith species are present in the system at time t. The $s \times 1$ vector n, with elements n_i, is thus a sample (or a value) of the stochastic process $N(t)$.

We can also describe the system state at time t by the $s \times 1$ vector $X(t)$ whose ith element is the concentration $X_i(t)$ of the ith component. The concentration $X_i(t)$ is, in general, the copy number $N_i(t)$ divided by some fixed scaling parameter Ω_i specific to that component. In other words

$$N_i(t) = \Omega_i X_i(t), \quad n_i = \Omega_i x_i \,.$$

Each concentration $X_i(t)$ is a stochastic process, where $X_i(t) = x_i$ means that the concentration of the ith component at time t is x_i. The $s \times 1$ vector x, with elements x_i, is thus a sample of the stochastic process $X(t)$. The copy number and concentration (vectors) are related by

$$N(t) = \Omega \odot X(t), \quad n = \Omega \odot x,$$

where Ω is the $s-$vector of elements Ω_i and the binary operation $\odot$ denotes the element-wise multiplication.

Commonly, all components are scaled by a single parameter, in which case Ω is a scalar known as the *system size.* A common choice for the system size is some multiple of the volume V of the system. For molar concentrations, the system size chosen is $\Omega = N_A V$ where N_A is the Avogadro's constant. In systems biology, one often uses relative concentrations x_i where Ω_i is some fixed copy

Accepted manuscript

ACCEPTED MANUSCRIPT

number specific to component i. The simplest case of relative concentrations uses a single (maximum) copy number $n_{\max}$ for all components. Note, however, that the approach developed here allows for relative concentrations instead of assuming one global system-size Ω as done in [16, 51, 53, 54, 64].

If we assume that the molecules are well mixed and are available everywhere for a reaction (space can be ignored), then the probability of a reaction in a short time interval depends almost entirely on the most recent copy numbers (and not its earlier values). In other words, the stochastic process $N(t)$ of copy numbers is *Markovian* in continuous-time. Since changes in the copy numbers require the occurrences of reactions which are discrete event phenomena, $N(t)$ is referred as a *jump process*. The Markov property implies that each reaction channel j can be characterised by a *reaction propensity* $a_j(n)$ defined such that, in state n, the probability of one occurrence of reaction channel j in a vanishingly short time interval of length dt is $a_j(n)dt$.

The stochastic process $N(t)$ is characterised by the (time-dependent) probability distribution $P(n,t) = \Pr[N(t) = n]$, starting from some initial distribution $P(n,0)$ as in [58]. Usually, the initial state is assumed to be known (as in [44]), $N(0) = n^0$ so that $P(n^0, 0) = 1$ and $P(n, 0) = 0$ for all $n \neq n^0$. In that case the distribution can be interpreted as a time-dependent transition probability

$$P(n,t) = \Pr\Big[N(t) = n \,|\, N(0) = n^0\Big]$$

of moving from the fixed initial state n^0 to the state n at time t. The probability distribution itself is characterised by its moments. The transition from state n to the state determined by the jth reaction will be represented by the following scheme

$$n \xrightarrow{a_j(n)} n + S_{\bullet j}$$

where $S_{\bullet j}$ is the jth column of the *stoichiometry matrix* S whose element S_{ij} denotes the change in copy number of the ith component resulting from the occurrence of the jth channel. Similarly the transitions towards state n from the state determined by the jth reaction can be represented by

$$n - S_{\bullet j} \xrightarrow{a_j(n - S_{\bullet j})} n$$

where the argument of the propensity function a_j is $n - S_{\bullet j}$ which is the assumed current state. Transitions away from state n will decrease the probability $P(n,t)$ while those towards state n will increase it. Since this is equally true for each reaction channel, during a short time interval of length Δt, the change in the probability is given by

$$P(n, t+\Delta t) - P(n,t) = \sum_{j=1}^{r} P(n - S_{\bullet j}, t) a_j(n - S_{\bullet j}) \Delta t - \sum_{j=1}^{r} P(n,t) a_j(n) \Delta t + o(\Delta t)$$

where $o(\Delta t)$ represents terms that vanish faster than Δt as the later approaches zero. As Δt approaches zero in the above system of equations, we are led to

Accepted manuscript

ACCEPTED MANUSCRIPT

what is known as the *chemical master equation* (CME):

$$\frac{d}{dt}P(n,t) = \sum_{j=1}^{r}\Big[a_j(n - S_{\bullet j})P(n - S_{\bullet j}, t) - a_j(n)P(n,t)\Big], \tag{1}$$

subject to the initial condition: $P(n^0, 0) = 1$ and $P(n, 0) = 0$ for all $n \neq n^0$. We will switch between the two alternative notations $\frac{d}{dt}\phi(t)$ and $\frac{d\phi}{dt}$ for any scalar quantity $\phi(t)$. We will prefer the later when dependence on time variable is implicitly clear.

Since there is one equation for each state n and there is potentially a large number of possible states, it is impractical to solve the CME. In most cases, we are interested in the first two-moments: component-wise copy number means

$$\langle N_i(t)\rangle = \sum_n n_i P(n,t),$$

and the covariances

$$\langle N_i, N_k\rangle = \Big\langle \big(N_i - \langle N_i\rangle\big)\big(N_k - \langle N_k\rangle\big)\Big\rangle,$$

between copy numbers of component pairs. These covariances form the covariance matrix in which the diagonal elements are component-wise variances.

In the present paper, we are interested in the mean concentration vector $\mu(t)$ with elements

$$\mu_i(t) = \langle X_i(t)\rangle = \frac{\langle N_i(t)\rangle}{\Omega_i}$$

and the concentration covariance matrix $\sigma(t)$ with elements

$$\sigma_{ik}(t) = \langle X_i(t), X_k(t)\rangle = \frac{\langle N_i(t), N_k(t)\rangle}{\Omega_i\Omega_k}$$

Hereafter, we leave out the dependence on time to simplify the notation, but include it occasionally when causing confusion.

2.1. Continuous approximations of the jump process $N(t)$

Although the stochastic simulation algorithm and its extensions provide a way to generate sample paths of copy numbers for a biochemical system, there is a significant computational burden. Characterisation of the probability distribution in terms of its moments requires a large number of simulations runs. To that end, attempts have been made towards approximations of the CME, the most notable being the chemical Langevin equation (CLE) by Gillespie [46] (see also [58]). He obtained that continuous approximation for the incremental change $\Delta N = N(t+\Delta t) - N(t)$ in copy number during a short interval $[t, t+\Delta t]$ where the interval length Δt satisfies two conditions: (i) It is small enough that the propensity does not change "appreciably" during the interval, and (ii) is large enough that the expected number of occurrences $\langle Z_j(t+\Delta t) - Z_j(t)\rangle$ of

Accepted manuscript

ACCEPTED MANUSCRIPT

each reaction channel j during the interval is much larger than unity. That continuous approximation takes the form of the CLE (derived in Appendix A)

$$\Delta N_i = \sum_{j=1}^{r} S_{ij} a_j\left(N\right) \Delta t + \sum_{j=1}^{r} S_{ij} \sqrt{a_j\left(N\right)} \mathcal{N}_j \sqrt{\Delta t}. \tag{2}$$

where $\{\mathcal{N}_j(t)\}$ is a set of r statistically independent standard Gaussian random processes (with zero mean and unit variance). An alternative form of CLE (derived in Appendix A) is

$$\Delta N = S\, a\left(N\right) \Delta t + \Big(D\left(N\right)\Big)^{1/2} \mathcal{N} \sqrt{\Delta t} \tag{3}$$

where $\mathcal{N}(t)$ is an $s \times 1$ vector of statistically independent standard Gaussian random processes and $D^{1/2}$ is the matrix square root of the diffusion matrix

$$D(n) = S\, \mathrm{diag}\left(a_1(n), \ldots, a_r(n)\right)\, S^T, \tag{4}$$

where the superscript T represents the transpose of a matrix and $\mathrm{diag}\left(a_1, \ldots, a_r\right)$ is the diagonal matrix with elements $a_1, \ldots, a_r$ on the diagonal. The probability density function $P^c(n,t)$ of the continuous Markov process obeys the (forward) Fokker-Planck equation (FPE) [46, 65]

$$\frac{\partial}{\partial t} P^c(n,t) = \sum_{j=1}^{r} \Big(- \sum_{i=1}^{s} S_{ij} \frac{\partial}{\partial n_i} + \frac{1}{2} \sum_{i,k=1}^{s} S_{ij} S_{kj} \frac{\partial^2}{\partial n_i \partial n_k} \Big) \left[a_j(n) P^c(n,t) \right]. \tag{5}$$

In effect, condition (i) allows a Poissonian approximation of $Z_j(t+\Delta t) - Z_j(t)$ and condition (ii) allows a normal approximation of the Poissonian. The two conditions seem conflicting and require the existence of a domain of macroscopically infinitesimal time intervals. Although the existence of a such a domain cannot be guaranteed, Gillespie argues that this can be found for most practical cases. Admitting that, "it may not be easy to continually monitor the system to ensure that conditions (i) and (ii) [..] are satisfied." He justifies his argument by saying that this "will not be the first time that Nature has proved to be unaccommodating to our purposes." [46].

Generating sample paths of (2) is orders of magnitude faster than doing the same for the CME because it essentially needs generation of normal random numbers. See [66] for numerical simulation methods of stochastic differential equations such as (2) and (3). The choice between (2) and (3) may be dictated by the number of reactions r relative to the number of species s because, in each simulation step, the former requires r random numbers whereas the latter requires s random numbers. However, solving the nonlinear FPE (5) for the probability density is as difficult as the CME. Therefore, on the analytical side, the CLE and the associated nonlinear FPE do not provide any significant advantage. That leads to a further simplification referred to as the *linear noise approximation* (LNA) [44, 45]. The LNA is a linear approximation of the nonlinear FPE (5) obtained by linearising the propensity function around the mean.

Accepted manuscript

ACCEPTED MANUSCRIPT

The solution of the LNA is a Gaussian distribution with a mean that is equal to the solution of the deterministic ODE model and a covariance matrix that obeys a linear ODE. That is the main drawback of LNA because, for a system containing at least one bimolecular reaction, the mean of a stochastic model is not equal to the solution of deterministic ODEs, as shown next.

2.2. Mean of the stochastic model

The mean copy number for the ith component obeys the ODE

$$\frac{d\langle N_i\rangle}{dt} = \sum_{j=1}^{r} S_{ij}\left\langle a_j\big(N\big)\right\rangle \tag{6}$$

which is derived in Appendix B. In general, the expectation on the right of (6) involves involves the unknown probability distribution $P(n,t)$. In other words, the mean copy number depends not just on the mean itself, but also involves higher-order moments, and therefore (6) is, in general, not closed in the mean unless the reaction propensity is a linear function of N which is the case only for zero- and first-order reactions. Take the example of a first-order reaction $X \xrightarrow{k} Y$ with n denoting the copy number of its reactant and k denoting the reaction coefficient. The reaction propensity $a(n) = kn$ (mass action kinetics) is linear in n. From probability theory, the expectation becomes $\langle kN\rangle = k\langle N\rangle$ and thus we do not need to know the probability distribution for solving the ODE in the mean. Only when *all* reactions are *elementary* and are of zero or first-order, we have exact equations for the evolution of mean:

$$\frac{d\langle N_i\rangle}{dt} = \sum_{j=1}^{r} S_{ij} a_j\big(\langle N\rangle\big)\,.$$

This corresponds to the ODE system for the deterministic model, which treats the copy numbers $n(t)$ as a continuous time-varying quantity that can be uniquely predicted for a given initial condition. For systems containing second (and higher) order reactions, $a(n)$ is a nonlinear function and the evolution of the mean cannot be determined by the mean alone. Instead the mean depends on higher-order moments, and hence the deterministic ODE model and the LNA cannot be used to describe the mean in (6).

2.3. The 2MA approach

The present section provides only a brief outline of the 2MA approach and we refer to the Appendix B for a detailed derivation.

An exact and closed representation for the mean is not possible in general, as evident from (6). The same is true for (co)variance and higher-order moments. One way to solve this problem is by repeating many stochastic simulation runs based on CME or the CLE, and computing the desired moments from the ensemble runs. An alternative is to find approximations to the exact ODEs such as (6) for the moments. The 2MA is one such attempt which assumes closure to the

Accepted manuscript

ACCEPTED MANUSCRIPT

first two moments. A scheme of chemical reactions or a system of deterministic ODEs is the starting point. From this are concluded the reaction propensities $a_j(n)$ which appear as coefficients in the CME describing the time derivative of the probability distribution $P(n,t)$. By taking the first two-moments of the CME and subsequent simplifications followed by appropriate scaling, two sets of ODEs for the mean concentration vector $\mu(t)$ and covariance matrix $\sigma(t)$ are derived. This is followed by Taylor expansions of any nonlinear functions involving the propensity vector $a(n)$. Ignoring central moments of 3rd and order higher eventually leads to the 2MA system (derived in Appendix B):

$$\frac{d\mu_i}{dt} = f_i(\mu) + \frac{1}{2}\frac{\partial^2 f_i}{\partial x \partial x^T} : \sigma \tag{7}$$

$$\frac{d\sigma_{ik}}{dt} = \frac{\partial f_i}{\partial x^T}\sigma_{\cdot k} + \sigma_{i\cdot}\frac{\partial f_k}{\partial x} + \frac{1}{\sqrt{\Omega_i \Omega_k}}\left[B_{ik}(\mu) + \frac{1}{2}\frac{\partial^2 B_{ik}}{\partial x \partial x^T} : \sigma\right] \tag{8}$$

where $\sigma_{\cdot k}$ and $\sigma_{i\cdot}$ respectively denote the kth column and ith row of σ, all partial derivatives with respect to the state x are evaluated at $x = \mu$, and

$$\begin{aligned} f_i(x) &= \frac{1}{\Omega_i}\sum_{j=1}^{r} S_{ij} a_j(\Omega \odot x) \\ B_{ik}(x) &= \frac{1}{\sqrt{\Omega_i \Omega_k}}\sum_{j=1}^{r} S_{ij} S_{kj} a_j(\Omega \odot x)\,. \end{aligned} \tag{9}$$

Here the binary operation : denotes the Frobenius inner product, that is, the sum of products of the corresponding elements between two matrices. The *effective flux* on the right in (7) is the sum of a *deterministic flux* $f(\mu)$ and a *stochastic flux* $\frac{1}{2}\frac{\partial^2 f_i}{\partial x \partial x^T} : \sigma$, the latter determined by the dynamics of both the mean and (co)variance. This influence of the (co)variance implies that knowledge of fluctuations is important for a correct description of the mean. This also indicates an advantage of the stochastic framework over its deterministic counterpart: starting from the same assumptions and approximations, the stochastic framework allows us to describe the influence of fluctuations on the mean. This can be posed as the central phenomenological argument for stochastic modelling.

Note that (7) is exact for systems where no reaction has an order higher than two because then 3rd and higher derivatives of propensity are zero. In (8), the *drift matrix* $\partial f / \partial x^T$ reflects the noise dynamics for relaxation (dissipation) to the steady state and the (Taylor approximation to the 2nd order of) *diffusion matrix* $B(x)$ the randomness (fluctuation) of the individual events. These terms are borrowed from the *fluctuation-dissipation theorem* (FDT) [67, 68], which has the same form as (8). The scaling factor $1/\sqrt{\Omega_i \Omega_k}$, that becomes $1/\Omega$ for scalar Ω, confirms the inverse relationship between the noise, as measured by (co)variance, and the system size. Note the influence of the mean on the (co)variance in (8).

A deterministic model treats concentrations $x(t)$ as continuous variables that can be predicted entirely from the initial conditions. Hence there is no noise term in the deterministic model and the ODEs reduce to $\dot{x} = f(x)$.

Accepted manuscript

ACCEPTED MANUSCRIPT

Since the 2MA approach is based on the truncation of terms containing 3rd and higher-order moments, any conclusion from the solution of 2MA must be drawn with care. Ideally, the 2MA should be complemented and checked with a reasonable number of SSA runs.

In [53, 54], the 2MA has been applied to biochemical systems, demonstrating quantitative and qualitative differences between the mean of the stochastic model and the solution of the deterministic model. The examples used in [53, 54] all assume elementary reactions (and hence propensities at most quadratic) and the usual interpretation of concentration as the moles per unit volume. In the next section, we investigate the 2MA for complex systems with non-elementary and relative concentrations. The reason for our interest in non-elementary reactions is the frequent occurrence of rational propensities (reaction rates), say of Michaelis-Menten type or Hill type, in models in the system biology literature (e.g. [69]).

2.4. The link between the CLE and the 2MA

Consider the system in state $n = \Omega x$. The component-wise flux (appearing in the 2MA and defined in (9)) multiplied by the corresponding size parameter, $\Omega_i f_i(x)$, appears as the coefficient of Δt of the first term on the right of the CLE (2). Moreover, the (i, k)th element of concentration diffusion matrix B, appearing in (9), multiplied by the square root of the corresponding pair of size parameters, $\sqrt{\Omega_i \Omega_k} B_{ik}(x)$, turns out to be the element $D_{ik}(n)$ of the copy-number diffusion matrix $D(n)$ whose matrix square root $(D(n))^{1/2}$ appears as a coefficient in the noise term of the CLE (3). Essentially, both approaches approximate the Markov process by a Gaussian random process.

3. Fission yeast cell cycle modelling

The growth and reproduction of organisms requires a precisely controlled sequence of events known as the cell cycle [70]. On a coarse scale, the cell cycle is composed of four phases: the replication of DNA (S phase), the separation of DNA (mitosis, M phase), and the intervening phases (gapes G1 and G2) which allow for preparation, regulation and control of cell division. The central molecular components of cell cycle control system have been identified [70, 71].

Cell cycle experiments show that cycle times (CTs) have different patterns for the wild type and for various mutants [72, 73]. For the wild type, the CTs have more or less a constant value near 150 min ensured by a size control mechanism: mitosis happens only when the cell has reached a critical size. The value 150 min has been considered in [48, 64, 73, 74] as the CT of an average WT cell (also referred to as the "mass-doubling time"). The double-mutant of fission yeast (namely *wee1⁻ cdc25*Δ) exhibits quantised cycle times: the CTs get clustered into three different groups (with mean CTs of 90, 160 and 230 min). The proposed explanation for the quantised cycle times is a weakend positive feedback loop (due to wee1 and cdc25) which means cells reset (more than once)

Accepted manuscript

ACCEPTED MANUSCRIPT

back to G2 from early stages of mitosis by premature activation of a negative feedback loop [73, 74].

Many deterministic ODE models describing the cell cycle dynamics have been constructed [60, 62, 75, 76]. These models can explain many aspects of the cell cycle including the size control for both the wild type and mutants. Since deterministic models describe the behaviour of a non-existing 'average cell', neglecting the differences among cells in culture, they fail to explain curious behaviours such as the quantised cycle times in the double-mutant. To account for such curiosities in experiments, two stochastic models were constructed by Sveiczer: The first model [73, 74] introduces (external) noise into the rate parameter of the protein Pyp3. The second model [77] introduces noise into two cell and nuclear sizes after division asymmetry. Full stochastic models that treat all the time-varying protein concentrations as random variables are reported in [48, 64]. They provide a reasonable explanation for the size control in wild type and the quantised CTs in the double-mutant type. Both models employ the Langevin approach and hence require many simulation runs to provide an ensemble for computing the mean and (co)variance. However, the simulation results of stochastic models in [48, 64, 73, 74, 77] represent one trajectory (for a large number of successive cycles) of the many possible in the ensemble from which the CT statistics (time averages) are computed. We will see that the time-averages computed from the 2MA simulation are for the ensemble of all trajectories.

3.1. The deterministic model

We base our 2MA model on the deterministic ODE model for the fission yeast cell cycle, developed by Tyson-Novák in [60]. In this context, the cell cycle control mechanism centres around the M-phase promoting factor (MPF), the active form of the heterodimer Cdc13/Cdc2, and its antagonistic interactions with enemies (Ste9,Slp1,Rum1) and the positive feedback with its friend Cdc25. These interactions, among many others, define a sequence of check points to control the timing of cell cycle phases. The result is MPF activity oscillation between low (G1-phase), intermediate (S- and G2-phases) and high (M-phase) levels that is required for the correct sequence of cell cycle events. For simplicity, it is assumed that the cell divides functionally when MPF drops from 0.1.

Table 1 lists the proteins whose concentrations x_i, together with MPF concentration, are treated as dynamic variables that evolve according to

$$\frac{dx_i}{dt} = f_i^+(x) - f_i^-(x)\,. \tag{10}$$

Here $f_i^+(x)$ is the production flux and $f_i^-(x)$ is the elimination flux of ith protein. Note that the summands in the fluxes $f_i^+(x)$ and $f_i^-(x)$ are rates of reactions, most of which, are non-elementary (summarizing many elementary reactions into a single step). Quite a few of these reaction rates have rational expressions which requires the extended 2MA approach developed in this paper.

Accepted manuscript

ACCEPTED MANUSCRIPT

Table 1: Proteins and fluxes. Here x denotes the vector of concentrations x_1 to x_8.

Index i	Protein	Production flux $f_i^+(x)$	Elimination flux $f_i^-(x)$
1	Cdc13_T	$k_1 M$	$(k_2' + k_2'' x_3 + k_2''' x_5)\, x_1$
2	preMPF	$(x_1 - x_2)\, k_\text{wee}$	$(k_{25} + k_2' + k_2'' x_3 + k_2''' x_5)\, x_2$
3	Ste9	$\frac{(k_3' + k_3'' x_5)(1-x_3)}{J_3+1-x_3}$	$\frac{(k_4' x_8 + k_4 x_\text{mpf}) x_3}{J_4+x_3}$
4	Slp1_T	$k_5' + \frac{k_5'' x_\text{mpf}^4}{J_4^4 + x_\text{mpf}^4}$	$k_6 x_4$
5	Slp1	$k_7 \frac{(x_4 - x_5) x_6}{J_7 + x_4 - x_5}$	$k_6 x_5 + k_8 \frac{x_5}{J_8 + x_5}$
6	IEP	$k_9 \frac{(1-x_6) x_\text{mpf}}{J_9 + 1 - x_6}$	$k_{10} \frac{x_6}{J_{10} + x_6}$
7	Rum1_T	k_{11}	$(k_{12} + k_{12}' x_8 + k_2'' x_\text{mpf})\, x_7$
8	SK	$k_{13} x_\text{tf}$	$k_{14} x_8$

The MPF concentration x_mpf can be obtained from the algebraic relation

$$x_\text{mpf} = \frac{(x_1 - x_2)\,(x_1 - x_\text{trim})}{x_1} \tag{11}$$

where

$$\begin{aligned}
\frac{dM}{dt} &= \rho M \\
x_\text{trim} &= \frac{2 x_1 x_7}{\Sigma + \sqrt{\Sigma^2 - 4 x_1 x_7}} \\
x_\text{tf} &= G\left(k_{15} M, k_{16}', k_{16}'' x_\text{mpf}, J_{15}, J_{16}\right) \\
k_\text{wee} &= k_\text{wee}' + (k_\text{wee}'' - k_\text{wee}')\, G\left(V_\text{awee}, V_\text{iwee} x_\text{mpf}, J_\text{awee}, J_\text{iwee}\right) \\
k_{25} &= k_{25}' + (k_{25}'' - k_{25}')\, G\left(V_\text{a25} x_\text{mpf}, V_\text{i25}, J_\text{a25}, J_\text{i25}\right) \\
\Sigma &= x_1 + x_7 + K_\text{diss}, \\
G(a,b,c,d) &= \frac{2ad}{b - a + bc + ad + \sqrt{(b - a + bc + ad)^2 - 4(b-a)ad}}
\end{aligned} \tag{12}$$

Note that the cellular mass M is assumed to grow exponentially with a rate ρ, and the concentrations $(x_\text{trim}, x_\text{tf}, k_\text{wee}, k_{25})$ are assumed to be in a pseudo-steady-state to simplify the model. Note that we use a slightly different notation: ρ for mass growth rate (instead of μ), x_trim for Trimmer concentration and x_tf for TF concentration. We have to emphasise that the concentrations used in this model are relative and dimensionless. When one concentration is divided by another, the proportion is the same as a proportion of two copy numbers. Hence, such a concentration should not be interpreted as a copy number per unit volume (as misinterpreted in [64]). The parameters used in the Tyson-Novák model [60] are listed in Table 3 in Appendix D.

The deterministic ODE model describes the behaviour of an 'average cell', neglecting the differences among cells in culture. Specifically, it fails to explain

Accepted manuscript

ACCEPTED MANUSCRIPT

the experimentally observed clusters of the CT-vs-BM plot and the tri-modal distribution of CT [72–74, 77].

3.2. Feasibility of Gillespie simulations

Ideally, we should repeat many runs of Gillespie's SSA and compute our desired moments from the ensemble of those runs. At present, there are two problems which this. The first problem is the requirement of elementary reactions for SSA. The elementary reactions underlying the deterministic model [60] are not known. Many elementary steps have been simplified to obtain that model. Trying to perform an SSA on non-elementary reactions will lose the discrete event character of the SSA. The second problem arises from the fact that the SSA requires copy numbers which in turn requires knowledge of measured concentrations. All protein concentrations in the model are expressed in arbitrary units (a.u.) because the actual concentrations of most regulatory proteins in the cell are not known [63]. Tyson and Sveiczer[1] define relative concentration x_i of the ith protein as $x_i = n_i/\Omega_i$ where $\Omega_i = C_i N_A V$. Here C_i is an unknown characteristic concentration of the ith component. The idea is to make the relative concentrations x_i free of scale of the actual (molar) concentrations $n_i/N_A V$. Although one would like to vary C_i, this is computationally intensive. This problem is not so serious for the continuous approximations such as CLE, LNA and the 2MA which are all ODEs and can be numerically solved. Using Matlab R2009a on a quad-core 2.66 GHz CPU took longer than 10 hours to complete one SSA run of 465 cycles. According to a recently published report [78], to compare the stochastic results with the average behaviour, the simulation must be run thousands of times, for which the cited authors had to use a parallel super computer. The main focus of the present paper is the analytical 2MA.

3.3. The stochastic model using Langevin's approach

In [64] a stochastic model is proposed that replaces the ODE model (10) with a set of chemical Langevin equations (CLEs)

$$\frac{d}{dt}x_i(t) = f_i^+\big(x(t)\big) - f_i^-\big(x(t)\big) + \frac{1}{\Omega}\left[\sqrt{f_i^+\left(x(t)\right)}\Gamma_i^+(t) - \sqrt{f_i^-\left(x(t)\right)}\Gamma_i^-(t)\right],$$

which uses the Langevin noise terms: White noises Γ_i^+ and Γ_i^- scaled by $\sqrt{f_i^+(x)}$ and $\sqrt{f_i^-(x)}$ to represent the internal noise. The system parameter Ω has been described as the volume by the author. As we discussed before, the concentrations are relative levels with different system size parameters. That means that concentrations are not the same as copy numbers per unit volume.

[1] Personal communication.

Accepted manuscript

ACCEPTED MANUSCRIPT

Another stochastic model, employing the Langevin's approach, is reported in [48]. It approximates the squared noise amplitudes by linear functions:

$$\frac{d}{dt}x_i(t) = f_i\left(x(t)\right) + \sqrt{2D_i x_i(t)}\Gamma_i(t),$$

where D_i is a constant. The model dynamics $f(x)$ are missing in the noise term because the author wanted to represent both the internal and external noise by the second term on the right.

3.4. The 2MA model

For the cell cycle model, the flux f and the diffusion matrix B, defined in (9), have elements

$$f_i(x) = f_i^+(x) - f_i^-(x), \quad B_{ik}(x) = \begin{cases} f_i^+(x) + f_i^-(x) & \text{if } i = k \\ 0 & \text{if } i \neq k\,. \end{cases}$$

The off-diagonal elements of B are zero because each reaction changes only one component, so that $S_{ij}S_{kj} = 0$ for $i \neq k$. Once these quantities are known, it follows from (7) and (8) that the following set of ODEs:

$$\frac{d\mu_i}{dt} = f_i(\mu) + \frac{1}{2}\frac{\partial^2 f_i}{\partial x \partial x^T} : \sigma \tag{13}$$

$$\frac{d\sigma_{ii}}{dt} = 2\sum_l \frac{\partial f_i}{\partial x_l}\sigma_{li} + \frac{1}{\Omega_i}\left[B_{ii}(\mu) + \frac{1}{2}\frac{\partial^2 B_{ii}}{\partial x \partial x^T} : \sigma\right] \tag{14}$$

$$\frac{d\sigma_{ik}}{dt} = \sum_l \left[\frac{\partial f_i}{\partial x_l}\sigma_{lk} + \sigma_{il}\frac{\partial f_k}{\partial x_l}\right] \quad i \neq k \tag{15}$$

approximates (correctly to the 2nd order moments) the evolution of component-wise concentration mean and covariance. See See Tables 4-6 in Appendix D for the respective expressions of the drift matrix A, the stochastic flux ε_f and the correction-term ε_B added to the diffusion matrix B in (14).

Having at hand the moments involving the eight dynamic variables x_1 to x_8, the mean MPF concentration can be shown to be approximately (correct to 2nd order moments):

$$\mu_{\text{mpf}} = \mu_1 - \mu_2 - x_{\text{trim}} + \frac{x_{\text{trim}}}{\mu_1}\left[\left(1 + \frac{\sigma_{11}}{\mu_1^2}\right)\mu_2 - \frac{\sigma_{12}}{\mu_1}\right] \tag{16}$$

for the mean MPF concentration with the understanding that x_{trim} is in pseudo steady state (See Appendix C for the derivation). This expression for the average MPF activity demonstrates the influence of (co)variance on the mean as emphasised here. We see the dependence of mean MPF concentration μ_{mpf} on the variance σ_{11} and covariance σ_{12} in addition to the means μ_1, μ_2 and x_{trim}.

Accepted manuscript

ACCEPTED MANUSCRIPT

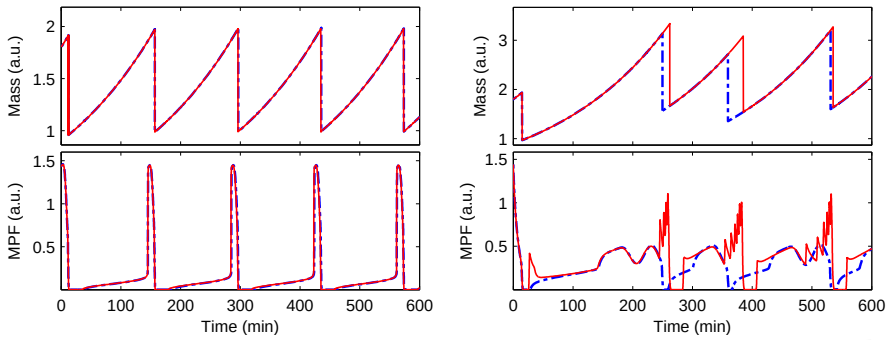

(a) (b)

Figure 1: The time-courses of mass and MPF activity: (a) for the wild type, (b) for the double-mutant type. The 2MA predicted mean trajectories are plotted as solid lines and the corresponding deterministic trajectories as dashed lines. The difference between the two predictions is negligible for the wild type, but significant for double-mutant type.

3.5. Simulations of the 2MA model

The system of ODEs (13)-(15) was solved numerically by the MATLAB solver ode15s [79]. The solution was then combined with algebraic relations (16). For parameter values, see Table 3. Since information about the individual scaling parameters Ω_i used in the definition of concentrations is not available, we have used $\Omega_i = 5000$ for all i. This value has also been used in [64], although there is no clear justification. Note, however, that the 2MA approach developed here will work for any combination of $\{\Omega_i\}$. The time-courses of mass and MPF activity are plotted in Figure 1a for the wild type and in Figure 1b for the double-mutant type. For the wild type, the 2MA predicted mean trajectories do not differ considerably from the corresponding deterministic trajectories. Both plots show a more or less constant CT near 150 min. Thus internal noise does not seem to have a major influence for the wild type.

For the double-mutant type, the difference between the 2MA and deterministic predictions is significant. The deterministic model (10) predicts alternating short cycles and long cycles because cells born at the larger size have shorter cycle, and smaller newborns have longer cycles [60]. This strict alternation due to size control is not observed in experiments: cells of same mass may have short or long cycles (excluding very large cells that have always the shortest CT) [72, 74]. This lack of size control is reproduced by the 2MA simulations: the multiple resettings of MPF to G2, induced by the internal noise, result in longer CTs (thus accounting for the 230-min cycles observed experimentally). Such MPF resettings have been proposed in [73, 74] to explain quantised CTs. No such resetting is demonstrated by the deterministic model.

Note that the mean $\mu(t)$ of the 2MA describes the average of an ensemble of

ACCEPTED MANUSCRIPT

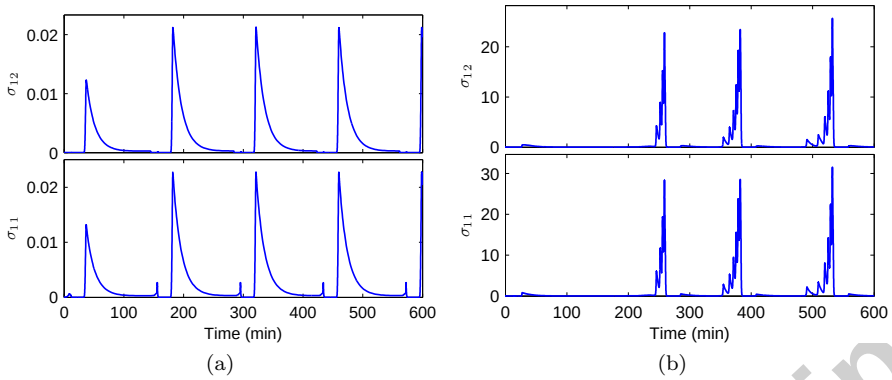

Figure 2: Variance σ_{11} (of Cdc13$_{\mathrm{T}}$) and covariance σ_{12} (between Cdc13$_{\mathrm{T}}$ and preMPF): (a) for the wild type, (b) for double-mutant type.

cells. Yet the MPF resettings observed in Figure (1b), near G2/M transition, introduce the required variability that explains the clustering of the cycle time observed in experiments. This is in contrast to the alternative stochastic approaches in [48, 64, 73, 74, 77] that use one sample trajectory rather than the ensemble average.

How do we explain this significant effect of noise for the double-mutant on one hand and its negligible effect for the wild type on the other hand? If we look at expression (16), we see the influence of the variance σ_{11} (of Cdc13$_{\mathrm{T}}$) and covariance σ_{12} (between Cdc13$_{\mathrm{T}}$ and preMPF) on the mean MPF concentration μ_{mpf}. The two (co)variances are plotted in Figure 2a for the wild type and in Figure 2b for the double-mutant type. It is clear that the two (co)variances have very small peaks for the wild type compared to the large peaks for the double-mutant type. Note that the larger peaks in Figure 2b are located at the same time points where the MPF activity exhibits oscillations and hence multiple resettings to G2. This suggest that the oscillatory behaviour of MPF near the G2/M transition is due to the influence of the oscillatory (co)variances. This coupling between the mean and (co)variance is not captured by the deterministic model.

It has to be realised that the above proposition requires validation since the 2MA approach ignores 3rd and higher-order moments. We cannot know whether that truncation is responsible for the oscillations in Figures 1 and 2, unless compared with a few sample trajectories simulated by the SSA. However, as discussed before, the SSA cannot be performed (at present) for the model in consideration. Therefore we need to compare the 2MA predictions for the double-mutant type cells with experimental data. Towards that end, values of cycle time (CT), birth mass (BM) and division mass (DM) were computed for 465 successive cycles of double-mutant cells. Figure 3 shows the CT-vs-BM plot and the CT distribution for three different values $\{5000, 5200, 5300\}$ of system

Accepted manuscript

ACCEPTED MANUSCRIPT

Table 2: Statistics over 465 successive cell cycles of the double-mutant type cells, predicted by the 2MA model, compared with experimental data, see [72, Table 1].

Case	μ_{CT}	σ_{CT}	$\mathrm{CV}_{\mathrm{CT}}$	μ_{DM}	σ_{DM}	$\mathrm{CV}_{\mathrm{DM}}$	μ_{BM}	σ_{BM}
(1)	131	47	0.358	2.22	0.45	0.203	1.21	0.24
(2)	138.8	12.4	0.09	3.18	0.101	0.0319	1.59	0.0575
(3)	138.8	17.6	0.127	3.25	0.178	0.055	1.623	0.0934
(4)	138.8	23.9	0.172	3.32	0.231	0.0697	1.657	0.12

(1) experimental data, (2) $\Omega = 5000$, (3) $\Omega = 5200$, (4) $\Omega = 5300$.

size Ω.

To make this figure comparable with experimental data from [72, 73], we assume that 1 unit of mass corresponds to 8.2 μm cell length [74]. We can see the missing size control (CT clusters), in qualitative agreement with experimentally observed ones (see [72, Figure 6] and [73, Figure 5] for a comparison). There are more than four clusters, which may have arisen from the truncated higher-order moments. The extreme value of CT higher than 230 min suggests more than two MPF resettings. Furthermore, more than three modes in the CT distribution may have arisen from the truncated higher-order moments. Table 2 compares the statistics for the double-mutant type cells, computed with the 2MA approach, with data from [72, Table 1]. Column 2-4 tabulate, for CT, the mean μ_{CT}, the standard deviation σ_{CT} and the coefficient of variation $\mathrm{CV}_{\mathrm{CT}}$, respectively. The other columns tabulate similar quantities for the division mass (DM) and the birth mass (BM). We see that only the mean CT is in agreement with the experimental data. The mean values for both BM and DM are larger than the corresponding experimental values. The other statistics are much smaller the corresponding experimental values. This and the above plots suggest that the 2MA should be used with caution. However, another aspect of the cell cycle model deserves attention here. The way the relative protein concentrations have been defined implies unknown values of the scaling parameters $\{\Omega_i\}$. Since $\Omega_i = C_i N_A V$, knowing the volume V does not solve the problem: the characteristic concentrations $\{C_i\}$ are still unknown. Our simulations have chosen typical values $\Omega = \{5000, 5200, 5300\}$. The corresponding three pairs of plots in Figure 3 and rows in Table 2 demonstrate a dependence of the results on a suitable system size. There is no way to confirm these values. The scaling parameters could be varied in a wider range in order to improve simulation accuracy, which we leave for future work. The conclusion is that the quantitative disagreement of the 2MA predictions can be attributed to two factors: 1) the truncated higher-order moments during the derivation of the 2MA, and (2) the unknown values of scaling parameters.

Accepted manuscript

ACCEPTED MANUSCRIPT

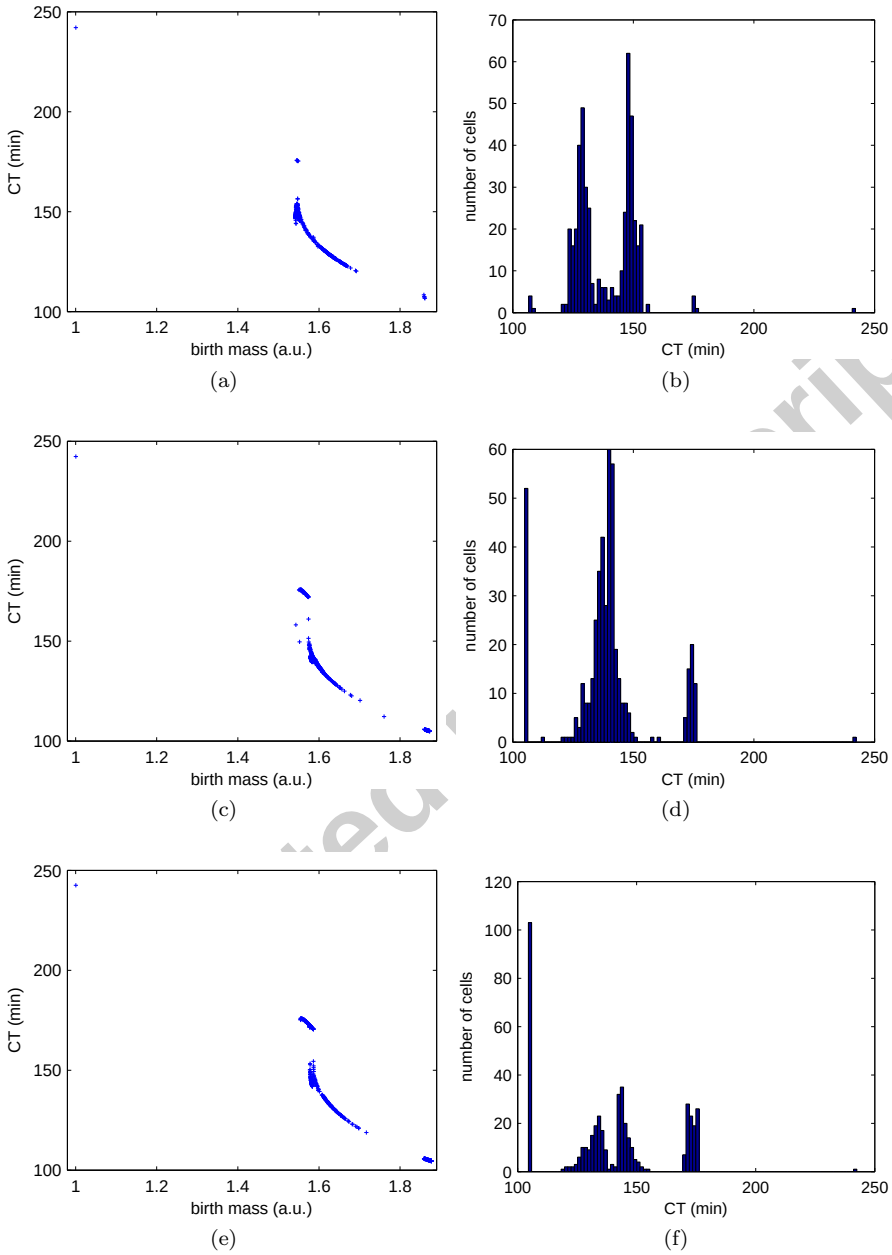

Figure 3: Cycle time behaviour over 465 successive cycles of the double-mutant cells, predicted by the 2MA model. (a,c,e): CT vs BM, (b,d,f): CT distribution, (a,b): $\Omega = 5000$, (c,d): $\Omega = 5200$, (e,f): $\Omega = 5300$. The plots are in qualitative agreement to experiments, see [72, Figure 6] and [73, Figure 5] for comparison.

ACCEPTED MANUSCRIPT

4. Conclusions

The recently developed two-moment approximation (2MA) [53, 54] is a promising approach because it accounts for the coupling between the means and (co)variances. We here extended the derivation of the 2MA to biochemical networks and established two advances to previous efforts: a) relative concentrations and b) non-elementary reactions. Both aspects are important in systems biology where one is often forced to aggregate elementary reactions into single step reactions. In these situations one cannot assume knowledge of elementary reactions to formulate a stochastic model. Previous derivations assumed elementary reactions and absolute concentrations. However, numerous existing models in systems biology use relative concentrations.

We investigated the applicability of the 2MA approach to the well established fission yeast cell cycle model. The simulations of the 2MA model show oscillatory behaviour near the G2/M transition, which is significantly different from the simulations of deterministic ODE model. One notable aspect of our analytical model is that, although it describes the average of an ensemble, it reproduces enough variability among cycles to reproduce the curious quantised cycle times observed in experiments on double mutants.

Acknowledgements

In the process of preparing this manuscript discussions with Hanspeter Herzel (Humboldt University), Akos Sveiczer (Budapest University of Technology & Economics) and Kevin Burrage (University of Queensland, Brisbane) helped in clarifying questions related to the cell cycle and stochastic modelling. We very much appreciate their willingness to have these discussions with us. M.U. has been supported by the Deutsche Forschungsgemeinschaft (DFG) through grant (WO 991/3-1). O.W. acknowledges support by the Helmholtz Alliance on Systems Biology and the Stellenbosch Institute for Advanced Study (STIAS). We also received valuable comments by the reviewers. One anonymous reviewer was particularly helpful and motivated us to demonstrate the link between the CLE and the 2MA.

Appendix A. Derivation of alternative forms of the CLE

The progress of a particular reaction can be described by a quantity known as the *reaction count* (RC) or *degree of advancement*. We will write $Z_j(t)$ for the RC of the jth reaction, where $Z_j(t) = z_j$ means that the jth reaction has occurred z_j times during the interval $[0, t)$. In the same interval the jth reaction will contribute a change of $z_j S_{ij}$ molecules to the overall change in the copy number N_i of the ith component. Summing up contributions from all the reactions, the copy number can be expressed as

$$N_i(t) = N_i(0) + \sum_{j=1}^{r} S_{ij} Z_j(t)\,. \tag{17}$$

Accepted manuscript

ACCEPTED MANUSCRIPT

The copy number increment $\Delta N_i = N_i(t+\Delta t) - N_i(t)$ during a short time interval $[t, t+\Delta t]$ is then a linear combination

$$\Delta N_i = \sum_{j=1}^{r} S_{ij} \Delta Z_j, \tag{18}$$

of the short-time RC increments $\Delta Z_j = Z_j(t+\Delta t) - Z_j(t)$. Following Gillespie [46], suppose it is known that $N(t) = n$. Since all the probabilities and expectations in this appendix are conditional on $N(t) = n$, we will use a simplified notation, which will not explicitly indicate this conditionality. Then the short-time RC increment ΔZ_j has the probability distribution

$$\Pr\left[\Delta Z_j = z_j\right] = o(\Delta t) + \begin{cases} a_j(n)\Delta t & \text{if} \quad z_j = 1 \\ 1 - a_j(n)\Delta t & \text{if} \quad z_j = 0 \\ 0 & \text{if} \quad z_j > 1 \end{cases} \tag{19}$$

where $o(\Delta t)$ represents a quantity that vanishes faster than Δt as the later approaches zero. For a vanishingly small Δt, the above distribution approaches the Poisson distribution with mean and variance equal to $a_j(n)\Delta t$. If Δt is small enough that each reaction propensity $a_j(n)$ does not change "appreciably" during the interval, then ΔZ is approximately Poissonian with channel-wise mean

$$\langle \Delta Z_j \rangle \approx a_j(n)\Delta t, \tag{20}$$

and (co)variance

$$\langle \Delta Z_j, \Delta Z_l \rangle \approx \begin{cases} a_j(n)\Delta t & \text{if}\, j = l \\ 0 & \text{if}\, j \neq l, \end{cases} \tag{21}$$

between channel pairs. If Δt is large enough that each RC increment $\langle \Delta Z_j \rangle$ has a very large value, $a_j(n)\,\Delta t \gg 1$, then the Poissonian ΔZ_j can be approximated by a normal random variable with the same mean and variance $a_j(n)\Delta t$ for each reaction channel. Since any normal random variable can be written as a sum of its mean and the standard normal variable, scaled by its standard deviation, we can write the normal approximation as

$$\Delta Z_j \approx a_j(n)\Delta t + \left(a_j(n)\Delta t\right)^{1/2} \mathcal{N}_j(t), \tag{22}$$

where $\mathcal{N}_j(t)$ denotes the channel-wise standard normal process, all processes in the set $\{\mathcal{N}_j(t)\}$ being statistically independent. Inserting the above equation into (18) gives

$$\Delta N_i \approx \sum_{j=1}^{r} S_{ij} a_j(n)\Delta t + \sum_{j=1}^{r} S_{ij} \left(a_j(n)\Delta t\right)^{1/2} \mathcal{N}_j(t)\,.$$

Replacing the supposedly known n by $N(t)$ in the above equation gives the first form (2) of the CLE in the main text.

Accepted manuscript

ACCEPTED MANUSCRIPT

Being a linear combination of Gaussian variables ΔZ_j, the copy number increment ΔN is also Gaussian which can be written in the form

$$\Delta N \approx \langle \Delta N \rangle + \left\langle \Delta N, \Delta N^T \right\rangle^{1/2} \mathcal{N}(t), \tag{23}$$

which is a sum of the mean $\langle \Delta N \rangle$ and an $s \times 1$ standard Gaussian random vector $\mathcal{N}(t)$ scaled by the matrix square-root $\left\langle \Delta N, \Delta N^T \right\rangle^{1/2}$ of the covariance matrix $\left\langle \Delta N, \Delta N^T \right\rangle$. Combining (18) and (20) gives

$$\langle \Delta N_i \rangle = \sum_{j=1}^{r} S_{ij} \langle \Delta Z_j \rangle \approx \sum_{j=1}^{r} S_{ij} a_j(n) \Delta t$$

for the component-wise mean copy-number increment and

$$\langle \Delta N \rangle \approx S\, a(n) \Delta t \tag{24}$$

for the mean copy-number increment vector. The covariance matrix $\left\langle \Delta N, \Delta N^T \right\rangle$ can be expressed in terms of reaction counts in the following way. From (18) we get the pair-wise multiplication

$$\Delta N_i \Delta N_k = \sum_{j=1}^{r} \sum_{l=1}^{r} S_{ij} S_{kl} \Delta Z_j \Delta Z_l \,.$$

Combining the standard relation $\langle \Delta N_i, \Delta N_k \rangle = \langle \Delta N_i \Delta N_k \rangle - \langle \Delta N_i \rangle \langle \Delta N_k \rangle$ with (21) gives

$$\langle \Delta N_i, \Delta N_k \rangle = \sum_{j=1}^{r} \sum_{l=1}^{r} S_{ij} S_{kl} \langle \Delta Z_j, \Delta Z_l \rangle \approx \sum_{j=1}^{r} S_{ij} S_{kj} a_j(n) \Delta t$$

for the pair-wise covariance between copy-number increments. Introducing an $s \times s$ matrix D defined element-wise by

$$D_{ik}(n) = \sum_{j=1}^{r} S_{ij} S_{kj} a_j(n),$$

the copy-number covariance matrix and its matrix square root can be written in the form

$$\left\langle \Delta N, \Delta N^T \right\rangle \approx D(n) \Delta t, \quad \left\langle \Delta N, \Delta N^T \right\rangle^{1/2} \approx (D(n))^{1/2} (\Delta t)^{1/2} \,.$$

Substituting the above and (24) in (23) gives

$$\Delta N \approx S\, a(n) \Delta t + (D(n))^{1/2} \mathcal{N}(t) (\Delta t)^{1/2} \,. \tag{25}$$

Replacing the supposedly known n by $N(t)$ in the above proves (3) in the main text. Note that the matrix square root $D^{1/2}$ is such that $D = D^{1/2} \left(D^{1/2}\right)^T$ and can be found from the eigenvalue decomposition of D.

Accepted manuscript

ACCEPTED MANUSCRIPT

Appendix B. Derivation of the 2MA equations

The short-time reaction count increment has the channel-wise (conditional) mean

$$\langle \Delta Z_j \mid N(t) = n \rangle = a_j(n)\Delta t + o(\Delta t)\,. \tag{26}$$

The unconditional expectation can be obtained by summing up the conditional expectation, weighted by the probabilities $P(n,t)$, over all possible states n:

$$\langle \Delta Z_j \rangle = \big\langle a_j\big(N(t)\big)\big\rangle\, \Delta t + o(\Delta t),$$

which for vanishingly small Δt approaches the ODE

$$\frac{d}{dt}\langle Z_j(t)\rangle = \langle a_j\left(N(t)\right)\rangle\ . \tag{27}$$

Thus the mean propensity of a particular reaction can be interpreted as the *average reaction count per unit time*. Take the expectation on both sides of the conservation relation (17) to obtain

$$\frac{d}{dt}\langle N_i(t)\rangle = \sum_{j=1}^{r} S_{ij}\,\big\langle a_j\big(N(t)\big)\big\rangle$$

which proves (6) in the main text. It is interesting to note that the above ODE is a direct consequence of mass conservation (17) and the definition of propensity because we have not referred to the CME (which is the usual procedure) during our derivation.

Dividing (6) by Ω_i gives the ODE for the component mean concentration,

$$\frac{d}{dt}\mu_i(t) = \big\langle f_i\big(X(t)\big)\big\rangle\,, \tag{28}$$

where

$$f_i(x) = \frac{1}{\Omega_i}\sum_{j=1}^{r} S_{ij}a_j(\Omega \odot x)$$

is the total *flux* of component i in state x.

Suppose the propensity $a_j(n)$ is a smooth function and that central moments $\langle (N-\mu)^m\rangle$ of order higher than $m=2$ can be ignored. In that case, the Taylor series expansion of flux $f_i(x)$ around the mean is

$$f_i(x) = f_i(\mu) + \frac{\partial f_i}{\partial x^T}(x-\mu) + \frac{1}{2}(x-\mu)^T\frac{\partial^2 f_i}{\partial x \partial x^T}(x-\mu) + \cdots\,.$$

All partial derivatives with respect to the state x are evaluated at $x=\mu$. The first-order partial derivative here is the ith row of the Jacobian $\partial f/\partial x^T$. The 2nd-order partial derivative is the Hessian of f_i. Expectation of the 2nd term on the right is zero. Expectation of the 3rd term is the sum of products of corresponding elements of the Hessian $\frac{\partial^2 f_i}{\partial x \partial x^T}$ and the covariance matrix σ.

Accepted manuscript

ACCEPTED MANUSCRIPT

Denoting such an inner product between two matrices by : and ignoring terms involving 3rd and higher-order moments, the ODE (28) can be approximated by

$$\frac{d\mu_i}{dt} = f_i(\mu) + \frac{1}{2}\frac{\partial^2 f_i}{\partial x \partial x^T} : \sigma,$$

which proves the first set of 2MA equations (7) in the main text. Here the 2nd term on the right is the internal noise that arises from the discrete and random nature of chemical reactions. Note that this term has been derived from the CME instead of being assumed like external noise. This shows that knowledge of fluctuations (even if small) is important for a correct description of the mean. This also indicates an advantage of the stochastic framework over it deterministic counterpart: starting from the same assumptions and approximations, the stochastic framework allows us to see the influence of fluctuation on the mean. Note that the above equation is exact for systems where no reaction has an order higher than two because then 3rd and higher derivatives of propensity are zero.

Before we can see how the covariance σ evolves in time, let us multiply the CME with $n_i n_k$ and sum over all n,

$$\begin{aligned}
\sum_n n_i n_k \frac{dP(n,t)}{dt} &= \sum_n n_i n_k \sum_{j=1}^{r} \left[a_j(n - S_{\cdot j})P(n - S_{\cdot j}, t) - a_j(n)P(n,t)\right] \\
&= \sum_n \sum_{j=1}^{r} \Big[(n_i + S_{ij})\,(n_k + S_{kj})\, a_j(n)P(n,t) - n_i n_k a_j(n)P(n,t) \Big] \\
&= \sum_n \sum_{j=1}^{r} (n_k S_{ij} + n_i S_{kj} + S_{ij} S_{kj})\, a_j(n)P(n,t)
\end{aligned}$$

where dependence on time is implicit for all variables except n and S. Dividing by $\Omega_i \Omega_k$ and recognising sums of probabilities as expectations,

$$\frac{d\,\langle X_i X_k\rangle}{dt} = \langle X_k f_i(X)\rangle + \langle X_i f_k(X)\rangle + \frac{\langle B_{ik}(X)\rangle}{\sqrt{\Omega_i \Omega_k}}$$

where the *diffusion matrix* $B(x)$ has elements

$$B_{ik}(x) = \frac{1}{\sqrt{\Omega_i \Omega_k}} \sum_{j=1}^{r} S_{ij} S_{kj} a_j(\Omega \odot x)\,.$$

The relation $\sigma_{ik} = \langle X_i X_k\rangle - \mu_i \mu_k$ can be utilised to yield

$$\frac{d\sigma_{ik}}{dt} = \langle (X_k - \mu_k)\, f_i(X)\rangle + \langle (X_i - \mu_i)\, f_k(X)\rangle + \frac{\langle B_{ik}(X)\rangle}{\sqrt{\Omega_i \Omega_k}} \tag{29}$$

for the covariances between concentrations of component pairs. The argument of the first expectation in (29) has Taylor expansion

$$f_i(x)\,(x_k - \mu_k) = f_i(\mu)\,(x_k - \mu_k) + \frac{\partial f_i}{\partial x^T}(x - \mu)\,(x_k - \mu_k) + \cdots\,.$$

Accepted manuscript

ACCEPTED MANUSCRIPT

Expectation of the first term on the right is zero. Ignoring 3rd and higher-order moments, the first expectation in (29) is then

$$\langle (X_k - \mu_k)\, f_i(X) \rangle = \frac{\partial f_i}{\partial x^T} \sigma_{\bullet k}\,.$$

By a similar procedure, the second expectation in (29) is

$$\langle (X_i - \mu_i)\, f_k(X) \rangle = \sigma_{i\bullet} \frac{\partial f_k}{\partial x},$$

correct to 2nd-order moments. The element $B_{ik}(x)$ of the diffusion matrix has Taylor expansion

$$B_{ik}(x) = B_{ik}(\mu) + \frac{\partial B_{ik}}{\partial x^T}(x-\mu) + \frac{1}{2}(x-\mu)^T \frac{\partial^2 B_{ik}}{\partial x \partial x^T}(x-\mu) + \cdots\,.$$

Taking term-wise expectation, and ignoring 3rd and higher-order moments,

$$\langle B_{ik}(X) \rangle = B_{ik}(\mu) + \frac{1}{2} \frac{\partial^2 B_{ik}}{\partial x \partial x^T} : \sigma\,.$$

Summing up the three expectations above gives the approximation of (29) by

$$\frac{d\sigma_{ik}}{dt} = \frac{\partial f_i}{\partial x^T} \sigma_{\bullet k} + \sigma_{i\bullet} \frac{\partial f_k}{\partial x} + \frac{1}{\sqrt{\Omega_i \Omega_k}} \left[B_{ik}(\mu) + \frac{1}{2} \frac{\partial^2 B_{ik}}{\partial x \partial x^T} : \sigma \right],$$

which proves the 2nd set of 2MA equations (8) in the main text. Remember that (8) is exact for systems that contain only zero and first-order reactions because in that case the propensity is already linear.

Appendix C. Mean MPF concentration

To find the mean MPF concentration, we start with the MPF concentration

$$x_{\mathrm{mpf}} = (x_1 - x_2)\left(1 - \frac{x_{\mathrm{trim}}}{x_1}\right) = x_1 - x_2 - x_{\mathrm{trim}} + x_{\mathrm{trim}} \frac{x_2}{x_1}\,.$$

The ratio x_2/x_1 can be expanded around the mean,

$$\frac{x_2}{x_1} = \frac{1}{\mu_1} \frac{x_2}{1 + \frac{(x_1 - \mu_1)}{\mu_1}} = \frac{1}{\mu_1} \left[x_2 - \frac{(x_1 - \mu_1)\, x_2}{\mu_1} + \frac{(x_1 - \mu_1)^2\, x_2}{\mu_1^2} + \cdots \right].$$

Taking expectation on both sides,

$$\begin{aligned} \left\langle \frac{X_2}{X_1} \right\rangle &= \frac{1}{\mu_1} \left\langle \frac{X_2}{1 + \frac{(X_1 - \mu_1)}{\mu_1}} \right\rangle \\ &= \frac{1}{\mu_1} \left\langle X_2 - \frac{(X_1 - \mu_1)\, X_2}{\mu_1} + \frac{(X_1 - \mu_1)^2\, X_2}{\mu_1^2} + \cdots \right\rangle \\ &= \frac{1}{\mu_1} \left[\mu_2 - \frac{\sigma_{12}}{\mu_1} + \frac{\mu_2 \sigma_{11}}{\mu_1^2} \right]. \end{aligned}$$

Accepted manuscript

ACCEPTED MANUSCRIPT

Table 3: Parameter values for the Tyson-Novák cell cycle model of the fission yeast (wild type) [60]. All constants have units min^{-1}, except the Js, which are dimensionless Michaelis constants, and K_{diss}, which is a dimensionless equilibrium constant for trimer dissociation. For the double-mutant type, one makes the following three changes: $k''_{\text{wee}} = 0.3$, $k'_{25} = k''_{25} = 0.02$.

$k_{15} = 0.03$, $k'_2 = 0.03$, $k''_2 = 1$, $k'''_2 = 0.1$, $k'_3 = 1$, $k''_3 = 10$, $J_3 = 0.01$,
$k'_4 = 2$, $k_4 = 35$, $J_4 = 0.01$, $k'_5 = 0.005$, $k''_5 = 0.3$, $k_6 = 0.1$, $J_5 = 0.3$,
$k_7 = 1$, $k_8 = 0.25$, $J_7 = J_8 = 0.001$, $J_8 = 0.001$, $k_9 = 0.1$, $k_{10} = 0.04$,
$J_9 = 0.01$, $J_{10} = 0.01$, $k_{11} = 0.1$, $k_{12} = 0.01$, $k'_{12} = 1$, $k''_{12} = 3$, $K_{\text{diss}} = 0.001$,
$k_{13} = 0.1$, $k_{14} = 0.1$, $k_{15} = 1.5$, $k'_{16} = 1$, $k''_{16} = 2$, $J_{15} = 0.01$, $J_{16} = 0.01$,
$V_{\text{awee}} = 0.25$, $V_{\text{iwee}} = 1$, $J_{\text{awee}} = 0.01$, $J_{\text{iwee}} = 0.01$, $V_{\text{a25}} = 1$, $V_{\text{i25}} = 0.25$,
$J_{\text{a25}} = 0.01$, $J_{\text{i25}} = 0.01$, $k'_{\text{wee}} = 0.15$, $k''_{\text{wee}} = 1.3$, $k'_{25} = 0.05$, $k''_{25} = 5$, $\rho = 0.005$.

Finally, the mean MPF concentration follows from the expectation of x_{mpf} to be

$$\mu_{\text{mpf}} = \mu_1 - \mu_2 - x_{\text{trim}} + \frac{x_{\text{trim}}}{\mu_1}\left[\left(1 + \frac{\sigma_{11}}{\mu_1^2}\right)\mu_2 - \frac{\sigma_{12}}{\mu_1}\right],$$

thus proving (16) in the main text.

Appendix D. Parameters and coefficients of the 2MA equations

Accepted manuscript

ACCEPTED MANUSCRIPT

Table 4: Rows of the drift matrix of the 2MA cell cycle model.

i	$\frac{\partial f_i}{\partial x^T}$
1	$\left[-k_2' - k_2''\mu_3 - k_2'''\mu_5, 0, -k_2''\mu_1, 0, -k_2'''\mu_1, 0, 0, 0\right]$
2	$\left[k_{\text{wee}}, -k_{\text{wee}} - k_{25} - k_2' - k_2''\mu_3 - k_2'''\mu_5, -k_2''\mu_2, 0, -k_2'''\mu_2, 0, 0, 0\right]$
3	$\left[0, 0, -\frac{\left(k_4'\mu_8 + k_4\mu_{\text{mpf}}\right)J_4}{(J_4+\mu_3)^2} - \frac{\left(k_3' + k_3''\mu_5\right)J_3}{(J_3+1-\mu_3)^2}, 0, \frac{(1-\mu_3)k_3''}{J_3+1-\mu_3}, 0, 0, -\frac{k_4'\mu_3}{J_4+\mu_3}\right]$
4	$[0, 0, 0, -k_6, 0, 0, 0, 0]$
5	$\left[0, 0, 0, \frac{k_7 J_7 \mu_6}{(J_7+\mu_4-\mu_5)^2}, -k_6 - \frac{k_7 J_7 \mu_6}{(J_7+\mu_4-\mu_5)^2} - \frac{k_8 J_8}{(J_8+\mu_5)^2}, \frac{(\mu_4-\mu_5)k_7}{J_7+x_4-\mu_5}, 0, 0\right]$
6	$\left[0, 0, 0, 0, 0, -\frac{k_9 x_{\text{mpf}} J_9}{(J_9+1-\mu_6)^2} - \frac{k_{10} J_{10}}{(J_{10}+\mu_6)^2}, 0, 0\right]$
7	$\left[0, 0, 0, 0, 0, 0, -k_{12} - k_{12}'\mu_8 - k_2''\mu_{\text{mpf}}, -k_{12}'\mu_7\right]$
8	$\left[0, 0, 0, 0, 0, 0, 0, -k_{14}\right]$

Table 5: Stochastic flux, the 2nd-order term in the Taylor expansion of $f_i(x)$ around the mean.

i	$\frac{1}{2}\frac{\partial^2 f_i}{\partial x \partial x^T} : \sigma$
1	$-k_2''\sigma_{13} - k_2'''\sigma_{15}$
2	$-k_2''\sigma_{23} - k_2'''\sigma_{25}$
3	$\left[\frac{\left(k_4'\mu_8 + k_4\mu_{\text{mpf}}\right)J_4}{(J_4+\mu_3)^3} - \frac{\left(k_3' + k_3''\mu_5\right)J_3}{(J_3+1-\mu_3)^3}\right]\sigma_{33} - \frac{k_3'' J_3 \sigma_{35}}{(J_3+1-\mu_3)^2} - \frac{k_4' J_4 \sigma_{38}}{(J_4+\mu_3)^2}$
4	0
5	$\frac{k_7 J_7 \mu_6 (2\sigma_{45} - \sigma_{44} - \sigma_{55})}{(J_7+\mu_4-\mu_5)^3} + \frac{k_7 J_7 (\sigma_{46} - \sigma_{56})}{(J_7+\mu_4-\mu_5)^2} + \frac{k_8 J_8}{(J_8+\mu_5)^3}\sigma_{55}$
6	$\left[\frac{k_{10} J_{10}}{(J_{10}+\mu_6)^3} - \frac{k_9 \mu_{\text{mpf}} J_9}{(J_9+1-\mu_6)^3}\right]\sigma_{66}$
7	$-k_{12}'\sigma_{78}$
8	0

Accepted manuscript

ACCEPTED MANUSCRIPT

Table 6: The 2nd-order term in Taylor expansion of $B_{ii}(x)$ around the mean.

i	$\frac{1}{2}\frac{\partial^2 B_{ii}}{\partial x \partial x^T} : \sigma$
1	$k_2''\sigma_{13} + k_2'''\sigma_{15}$
2	$k_2''\sigma_{23} + k_2'''\sigma_{25}$
3	$-\left[\frac{\left(k_4'\mu_8+k_4\mu_{\mathrm{mpf}}\right)J_4}{(J_4+\mu_3)^3} + \frac{\left(k_3'+k_3''\mu_5\right)J_3}{(J_3+1-\mu_3)^3}\right]\sigma_{33} - \frac{k_3''J_3\sigma_{35}}{(J_3+1-\mu_3)^2} + \frac{k_4'J_4\sigma_{38}}{(J_4+\mu_3)^2}$
4	0
5	$\frac{k_7J_7\mu_6(2\sigma_{45}-\sigma_{44}-\sigma_{55})}{(J_7+\mu_4-\mu_5)^3} + \frac{k_7J_7(\sigma_{46}-\sigma_{56})}{(J_7+\mu_4-\mu_5)^2} - \frac{k_8J_8}{(J_8+\mu_5)^3}\sigma_{55}$
6	$-\left[\frac{k_{10}J_{10}}{(J_{10}+\mu_6)^3} + \frac{k_9\mu_{\mathrm{mpf}}J_9}{(J_9+1-\mu_6)^3}\right]\sigma_{66}$
7	$k_{12}'\sigma_{78}$
8	0

References

[1] J. Paulsson, J. Elf, Stochastic Modeling of Intracellular Kinetics, in: Z. Szallasi, J. Stelling, V. Periwal (Eds.), System Modeling in Cellular Biology, The MIT Press, 2006, pp. 149–176.

[2] C. V. Rao, D. M. Wolf, A. P. Arkin, Control, exploitation and tolerance of intracellular noise, Nature 420 (6912) (2002) 231–237. doi:10.1038/nature01258.

[3] J. Paulsson, Summing up the noise, Nature 427 (2004) 415–418. doi:10.1038/nature02257.

[4] M. Kaern, T. C. Elston, W. J. Blake, J. J. Collins, Stochasticity in gene expression: from theories to phenotypes, Nat. Rev. Genet. 6 (6) (2005) 451–464. doi:10.1038/nrg1615.

[5] J. M. Raser, E. K. O'Shea, Noise in gene expression: Origins, consequences, and control, Science 309 (5743) (2005) 2010–2013. doi:10.1126/science.1105891.

[6] J. M. Pedraza, A. van Oudenaarden, Noise Propagation in Gene Networks, Science 307 (5717) (2005) 1965–1969. doi:10.1126/science.1109090.

[7] N. V. Mantzaris, From single-cell genetic architecture to cell population dynamics: quantitatively decomposing the effects of different population heterogeneity sources for a genetic network with positive feedback architecture, Biophys. J. 92 (12) (2007) 4271–288. doi:10.1529/biophysj.106.100271.

[8] J. Ansel, H. Bottin, C. Rodriguez-Beltran, C. Damon, M. Nagarajan, S. Fehrmann, J. François, G. Yvert, Cell-to-Cell Stochastic Variation in Gene Expression Is a Complex Genetic Trait, PLoS Genet. 4 (4) (2008) e1000049. doi:10.1371/journal.pgen.1000049.

Accepted manuscript

ACCEPTED MANUSCRIPT

[9] T. Lipniacki, P. Paszek, A. Brasier, B. Luxon, M. Kimmel, Transcriptional stochasticity in gene expression, J. Theor. Biol. 238 (2006) 348–367. doi:10.1016/j.jtbi.2005.05.032.

[10] P. Paszek, Modeling stochasticity in gene regulation: Characterization in the terms of the underlying distribution function, Bull Math Biol 69 (2007) 1567–1601. doi:10.1007/s11538-006-9176-7.

[11] A. Becskei, B. B. Kaufmann, A. van Oudenaarden, Contributions of low molecule number and chromosomal positioning to stochastic gene expression, Nat. Genet. 37 (9) (2005) 937–944. doi:10.1038/ng1616.

[12] O. G. Berg, J. Paulsson, M. Ehrenberg, Fluctuations and Quality of Control in Biological Cells: Zero-Order Ultrasensitivity Reinvestigated, Biophys. J. 79 (3) (2000) 1228–1236.

[13] J. Levine, H. Y. Kueh, L. Mirny, Intrinsic fluctuations, robustness, and tunability in signaling cycles, Biophys. J. 92 (12) (2007) 4473–4481. doi:10.1529/biophysj.106.088856.

[14] J. Paulsson, Models of stochastic gene expression, Phys. Life Rev. 2 (2005) 157–75. doi:10.1016/j.plrev.2005.03.003.

[15] J. Elf, M. Ehrenberg, Fast evaluation of fluctuations in biochemical networks with the linear noise approximation, Genome Res. 13 (11) (2003) 2475–2484. doi:10.1101/gr.1196503.

[16] Y. Tao, Y. Jia, T. G. Dewey, Stochastic fluctuations in gene expression far from equilibrium: Omega expansion and linear noise approximation, J. Chem. Phys. 122 (12) (2005) 124108. doi:10.1063/1.1870874.

[17] Y. Zhang, H. Yu, M. Deng, M. Qian, Nonequilibrium Model for Yeast Cell Cycle (2006).

[18] M. Dogterom, S. Leibler, Physical aspects of the growth and regulation of microtubule structures, Phys. Rev. Lett. 70 (9) (1993) 1347. doi:10.1103/PhysRevLett.70.1347.

[19] J. Paulsson, M. Ehrenberg, Noise in a minimal regulatory network: plasmid copy number control, Quarterly Reviews Of Biophysics 34 (1) (2001) 1–59. doi:10.1017/S0033583501003663.

[20] H. Qian, From discrete protein kinetics to continuous Brownian dynamics: A new perspective, Protein Sci. 11 (1) (2002) 1–5.

[21] J. M. G. Vilar, H. Y. Kueh, N. Barkai, S. Leibler, Mechanisms of noise-resistance in genetic oscillators, Proc. Natl. Acad. Sci. U. S. A. 99 (9) (2002) 5988–5992. doi:10.1073/pnas.092133899.

[22] J. Elf, J. Paulsson, O. G. Berg, M. Ehrenberg, Near-critical phenomena in intracellular metabolite pools, Biophys. J. 84 (1) (2003) 154–170.

Accepted manuscript

ACCEPTED MANUSCRIPT

[23] H. E. Samad, M. Khammash, Intrinsic noise rejection in gene networks by regulation of stability, in: First International Symposium on Control, Communications and Signal Processing, 2004, pp. 187–190. doi:10.1109/ISCCSP.2004.1296252.

[24] M. Thattai, A. van Oudenaarden, Attenuation of noise in ultrasensitive signaling cascades, Biophys. J. 82 (6) (2002) 2943–2950.

[25] H. B. Fraser, A. E. Hirsh, G. Giaever, J. Kumm, M. B. Eisen, Noise Minimization in Eukaryotic Gene Expression, PLoS Biol. 2 (6) (2004) e137. doi:10.1371/journal.pbio.0020137.

[26] Y. Morishita, K. Aihara, Noise-reduction through interaction in gene expression and biochemical reaction processes, J. Theor. Biol. 228 (3) (2004) 315–325. doi:10.1016/j.jtbi.2004.01.007.

[27] J. Paulsson, M. Ehrenberg, Random signal fluctuations can reduce random fluctuations in regulated components of chemical regulatory networks, Phys. Rev. Lett. 84 (2000) 5447–5450. doi:10.1103/PhysRevLett.84.5447.

[28] G. Hornung, N. Barkai, Noise Propagation and Signaling Sensitivity in Biological Networks: A Role for Positive Feedback, PLoS Comput. Biol. 4 (1) (2008) e8. doi:10.1371/journal.pcbi.0040008.

[29] Y. Lan, G. A. Papoian, The interplay between discrete noise and nonlinear chemical kinetics in a signal amplification cascade, J. Chem. Phys. 125 (15) (2006) 154901. doi:10.1063/1.2358342.

[30] T. Shibata, M. Ueda, Noise generation, amplification and propagation in chemotactic signaling systems of living cells, Biosystems 93 (1-2) (2008) 126–132. doi:10.1016/j.biosystems.2008.04.003.

[31] C. Blomberg, Fluctuations for good and bad: The role of noise in living systems, Physics of Life Reviews 3 (2006) 133–161. doi:10.1016/j.plrev.2006.06.001.

[32] B. S. Chen, Y. C. Wang, On the attenuation and amplification of molecular noise in genetic regulatory networks, BMC Bioinformatics 7 (2006) 52. doi:10.1186/1471-2105-7-52.

[33] J. Hasty, J. Pradines, M. Dolnik, J. J. Collins, Noise-based switches and amplifiers for gene expression, Proc. Natl. Acad. Sci. U. S. A. 97 (5) (2000) 2075–2080. doi:10.1073/pnas.040411297.

[34] M. Yoda, T. Ushikubo, W. Inoue, M. Sasai, Roles of noise in single and coupled multiple genetic oscillators, J. Chem. Phys. 126 (11) (2007) 115101. doi:10.1063/1.2539037.

[35] J. Paulsson, O. Berg, M. Ehrenberg, Stochastic focusing: fluctuation-enhanced sensitivity of intracellular regulation, Proc. Natl. Acad. Sci. U. S. A. 97 (2000) 7148–7153. doi:10.1073ypnas.110057697.

Accepted manuscript

ACCEPTED MANUSCRIPT

[36] M. Samoilov, S. Plyasunov, A. P. Arkin, Stochastic amplification and signaling in enzymatic futile cycles through noise-induced bistability with oscillations, Proc. Natl. Acad. Sci. U. S. A. 102 (7) (2005) 2310–2315. doi:10.1073/pnas.0406841102.

[37] J. E. Ferrell, W. Xiong, Bistability in cell signaling: How to make continuous processes discontinuous, and reversible processes irreversible, Chaos: An Interdisciplinary Journal of Nonlinear Science 11 (1) (2001) 227–236. doi:10.1063/1.1349894.

[38] S. Aumaître, K. Mallick, F. Pétrélis, Noise-induced bifurcations, multiscaling and on–off intermittency, Journal of Statistical Mechanics: Theory and Experiment 2007 (07) (2007) P07016. doi:10.1088/1742-5468/2007/07/P07016.

[39] E. M. Ozbudak, M. Thattai, H. N. Lim, B. I. Shraiman, A. V. Oudenaarden, Multistability in the lactose utilization network of Escherichia coli, Nature 427 (6976) (2004) 737–740. doi:10.1038/nature02298.

[40] M. N. Artyomov, J. Das, M. Kardar, A. K. Chakraborty, Purely stochastic binary decisions in cell signaling models without underlying deterministic bistabilities, Proc. Natl. Acad. Sci. U. S. A. 104 (48) (2007) 18958–18963. doi:10.1073/pnas.0706110104.

[41] T. E. Turner, S. Schnell, K. Burrage, Stochastic approaches for modelling in vivo reactions, Comput. Biol. Chem. 28 (3) (2004) 165–178. doi:10.1016/j.compbiolchem.2004.05.001.

[42] K. Singer, Application of the theory of stochastic processes to the study of irreproducible chemical reactions and nucleation processes, Journal of the Royal Statistical Society. Series B (Methodological) 15 (1) (1953) 92–106.

[43] D. Gillespie, Exact stochastic simulation of coupled chemical reactions, The Journal of Physical Chemistry 81 (25) (1977) 2340–2361. doi:10.1021/jp993732q.

[44] N. v. Kampen, Stochastic Processes in Physics and Chemistry (Third Edition), Elsevier Amsterdam, Amsterdam, 2007.

[45] J. Goutsias, A hidden Markov model for transcriptional regulation in single cells, IEEE/ACM Trans Comput Biol Bioinform 3 (1) (2006) 57–71. doi:10.1109/TCBB.2006.2.

[46] D. Gillespie, The chemical Langevin equation, J. Chem. Phys. 113 (1) (2000) 297–306. doi:10.1063/1.481811.

[47] N. V. Kampen, The Langevin approach, in: Stochastic Processes in Physics and Chemistry (Third Edition), Elsevier, Amsterdam, 2007, pp. 219–243. doi:10.1016/B978-044452965-7/50012-X.

Accepted manuscript

ACCEPTED MANUSCRIPT

[48] R. Steuer, Effects of stochasticity in models of the cell cycle: from quantized cycle times to noise-induced oscillations, J. Theor. Biol. 228 (3) (2004) 293–301. doi:10.1016/j.jtbi.2004.01.012.

[49] J. Zamborszky, C. I. Hong, A. Csikasz Nagy, Computational Analysis of Mammalian Cell Division Gated by a Circadian Clock: Quantized Cell Cycles and Cell Size Control, J Biol Rhythms 22 (6) (2007) 542–553. doi:10.1177/0748730407307225.

[50] F. Hayot, C. Jayaprakash, The linear noise approximation for molecular fluctuations within cells, Physical Biology 1 (4) (2004) 205–210. doi:10.1088/1478-3967/1/4/002.

[51] M. Scott, B. P. Ingalls, Using the linear noise approximation to characterize molecular noise in reaction pathways, in: Proceedings of the AIChE Conference on Foundations of Systems Biology in Engineering (FOSBE), Santa Barbara, California, 2005. arXiv:http://www.math.uwaterloo.ca/ bingalls/Pubs/ScottFOSBE.pdf.

[52] M. Scott, B. Ingalls, M. Kaern, Estimations of intrinsic and extrinsic noise in models of nonlinear genetic networks, Chaos: An Interdisciplinary Journal of Nonlinear Science 16 (2) (2006) 026107. doi:10.1063/1.2211787.

[53] J. Goutsias, Classical versus stochastic kinetics modeling of biochemical reaction systems, Biophys. J. 92 (7) (2007) 2350–2365. doi:10.1529/biophysj.106.093781.

[54] C. A. Gómez-Uribe, G. C. Verghese, Mass fluctuation kinetics: capturing stochastic effects in systems of chemical reactions through coupled mean-variance computations, J. Chem. Phys. 126 (2) (2007) 024109. doi:10.1063/1.2408422.

[55] L. Ferm, P. Lötstedt, A. Hellander, A Hierarchy of Approximations of the Master Equation Scaled by a Size Parameter, Tech. Rep. 2007-011, Uppsala University, Department of Information Technology (Apr. 2007).

[56] Y. Dublanche, K. Michalodimitrakis, N. Kümmerer, M. Foglierini, L. Serrano, Noise in transcription negative feedback loops: simulation and experimental analysis, Molecular Systems Biology 2 (2006) 41. doi:10.1038/msb4100081.

[57] V. Shahrezaei, J. F. Ollivier, P. S. Swain, Colored extrinsic fluctuations and stochastic gene expression, Mol Syst Biol 4 (2008) 196. doi:10.1038/msb.2008.31.

[58] R. Tomioka, H. Kimura, T. J. Kobayashi, K. Aihara, Multivariate analysis of noise in genetic regulatory networks, J. Theor. Biol. 229 (4) (2004) 501–521. doi:10.1016/j.jtbi.2004.04.034.

Accepted manuscript

ACCEPTED MANUSCRIPT

[59] M. Tang, The mean and noise of stochastic gene transcription, J. Theor. Biol. 253 (2008) 271–280. doi:10.1016/j.jtbi.2008.03.023.

[60] B. Novák, Z. Pataki, A. Ciliberto, J. J. Tyson, Mathematical model of the cell division cycle of fission yeast, Chaos: An Interdisciplinary Journal of Nonlinear Science 11 (1) (2001) 277–286. doi:10.1063/1.1345725.

[61] B. Novák, K. Chen, J. Tyson, Systems biology of the yeast cell cycle engine (2005). doi:10.1007/b137123.

[62] J. J. Tyson, A. Csikasz-Nagy, B. Novák, The dynamics of cell cycle regulation, BioEssays 24 (12) (2002) 1095–1109. doi:10.1002/bies.10191.

[63] A. Csikász-Nagy, D. Battogtokh, K. C. Chen, B. Novák, J. J. Tyson, Analysis of a generic model of eukaryotic cell cycle regulation, Biophys. J. 90 (2006) 4361–4379. doi:10.1529/biophysj.106.081240.

[64] M. Yi, Y. Jia, J. Tang, X. Zhan, L. Yang, Q. Liu, Theoretical study of mesoscopic stochastic mechanism and effects of finite size on cell cycle of fission yeast, Physica A: Statistical Mechanics and its Applications 387 (1) (2008) 323–334. doi:10.1016/j.physa.2007.07.018.

[65] D. Gillespie, The multivariate Langevin and Fokker-Planck equations, American Journal of Physics 64 (10) (1996) 1246–1257. doi:10.1119/1.18387.

[66] D. J. Higham, An Algorithmic Introduction to Numerical Simulation of Stochastic Differential Equations, SIAM Review 43 (3) (2001) 525–546. doi:10.1137/S0036144500378302.

[67] J. Keizer, Statistical thermodynamics of nonequilibrium processes, Springer, Berlin, 1987.

[68] M. Lax, Fluctuations from the nonequilibrium steady state, Reviews of Modern Physics 32 (1) (1960) 25–64. doi:10.1103/RevModPhys.32.25.

[69] J. J. Tyson, K. C. Chen, B. Novák, Sniffers, buzzers, toggles and blinkers: dynamics of regulatory and signaling pathways in the cell, Curr. Opin. Cell Biol. 15 (2) (2003) 221–231. doi:10.1016/S0955-0674(03)00017-6.

[70] D. O. Morgan, The Cell Cycle: Principles of Control, Primers in Biology, New Science Press, 2007.

[71] P. Nurse, A Long Twentieth Century of the Cell Cycle and Beyond, Cell 100 (1) (2000) 71–78. doi:10.1016/S0092-8674(00)81684-0.

[72] A. Sveiczer, B. Novák, J. Mitchison, The size control of fission yeast revisited, J. Cell Sci. 109 (12) (1996) 2947–2957. arXiv:http://jcs.biologists.org/cgi/reprint/109/12/2947.pdf.

Accepted manuscript

ACCEPTED MANUSCRIPT

[73] A. Sveiczer, B. Novák, Regularities and irregularities in the cell cycle of the fission yeast, Schizosaccharomyces pombe (a review) (Jan. 2002).

[74] A. Sveiczer, A. Csikasz-Nagy, B. Gyorffy, J. J. Tyson, B. Novák, Modeling the fission yeast cell cycle: Quantized cycle times in wee1- cdc25Delta mutant cells, Proc. Natl. Acad. Sci. U. S. A. 97 (14) (2000) 7865–7870. doi:10.1073/pnas.97.14.7865.

[75] B. Novák, A. Csikasz-Nagy, B. Gyorffy, K. Chen, J. J. Tyson, Mathematical model of the fission yeast cell cycle with checkpoint controls at the G1/S, G2/M and metaphase/anaphase transitions, Biophys. Chem. 72 (1-2) (1998) 185–200. doi:10.1016/S0301-4622(98)00133-1.

[76] B. Novák, J. J. Tyson, Modelling the controls of the eukaryotic cell cycle, Biochem. Soc. Trans. 31 (Pt 6) (2003) 1526–1529.

[77] A. Sveiczer, J. J. Tyson, B. Novák, A stochastic, molecular model of the fission yeast cell cycle: role of the nucleocytoplasmic ratio in cycle time regulation, Biophys. Chem. 92 (1-2) (2001) 1–15. doi:10.1016/S0301-4622(01)00183-1.

[78] T.-H. Ahn, L. T. Watson, Y. Cao, C. A. Shaffer, W. T. Baumann, Cell Cycle Modeling for Budding Yeast with Stochastic Simulation Algorithms, Tr-08-23, Computer Science, Virginia Tech (2008). arXiv:http://eprints.cs.vt.edu/archive/00001051/.

[79] T. MathWorks. Matlab R2007b [online] (2007).

Accepted manuscript